ARCRL-TR-75-0168

INFRARED RESPONSE OF IMPURITY DOPED SILICON MOSFET'S:

Experimental Characterization of The Infrared Response of Gold-Doped Silicon MOSFET's (IRFET's)

Leonard Forbes, Ph.D.
Department of Electrical Engineering
University of Arkansas
Fayetteville, Arkansas 72701

1 February 1975

Semiannual Technical Report No. 1

Approved for public release: distribution unlimited

Sponsored by:

DEFENSE ADVANCED RESEARCH PROJECTS AGENCY-ARPA Order No. 2794

Monitored by:

AIR FORCE CAMBRIDGE RESEARCH LABORATORIES
AIR FORCE SYSTEMS COMMAND
UNITED STATES AIR FORCE
HANSCOM AFB, MASSACHUSETTS 01731

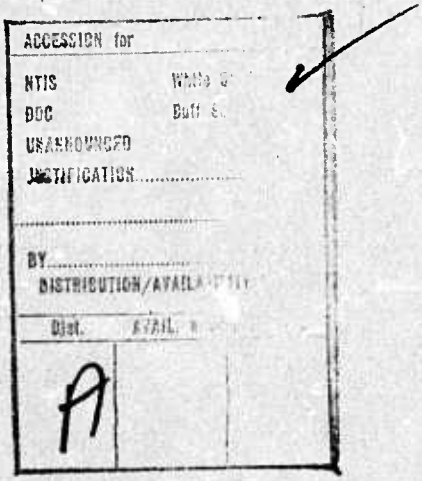

Qualified requestors may obtain additional copies from the Defense Documentation Center. All others should apply to the National Technical Information Service.

Unclassified

SECURITY CLASSIFICATION OF THIS PAGE (When Data Entered)

(18) (19) REPORT DOCUMENTATION PAGE

READ INSTRUCTIONS BEFORE COMPLETING FORM

1. REPORT NUMBER
AFCRL-TR-75-0168

(9) Semiannual Technical Rept. no. 1,

(6) Infrared Response of Impurity Doped Silicon MOSFET's: Experimental Characterization of the Infrared Response of Gold Doped Silicon MOSFET's (IRFET's).

5. TYPE OF REPORT & PERIOD COVERED
Scientific-Interim

6. PERFORMING ORG. REPORT NUMBER
Semiannual Tech No.1

7. AUTHOR(s)
(10) Leonard Forbes, Ph.D.

8. CONTRACT OR GRANT NUMBER(s)
(15) F19628-75-C-0071 + ARPA Order 2794

9. PERFORMING ORGANIZATION NAME AND ADDRESS
Dept. of Electrical Engineering
University of Arkansas
Fayetteville, Arkansas 72701

10. PROGRAM ELEMENT, PROJECT, TASK AREA & WORK UNIT NUMBERS
(16) AF-2794
61101E

11. CONTROLLING OFFICE NAME AND ADDRESS
Air Force Cambridge Research Laboratories
Hanscom AFB, Massachussetts 01731
Contract Monitor: Dr. Jacques E. Ludman/LOD

(11) 1 Feb 75

12. REPORT DATE

13. NUMBER OF PAGES
31

14. MONITORING AGENCY NAME & ADDRESS (if different from Controlling Office)

(12) 37p.

15. SECURITY CLASS. (of this report)
Unclassified

15a. DECLASSIFICATION DOWNGRADING SCHEDULE

16. DISTRIBUTION STATEMENT (of this Report)

Approved for public release; distribution unlimited

DDC RECEIVED JAN 2 1976 C

17. DISTRIBUTION STATEMENT (of the abstract entered in Block 20, if different from Report)

18. SUPPLEMENTARY NOTES

This Research was sponsored by the Defense Advanced Research Projects Agency, ARPA Order No. 2794.

19. KEY WORDS (Continue on reverse side if necessary and identify by block number)

Extrinsic Silicon Infrared Detectors.

20. ABSTRACT (Continue on reverse side if necessary and identify by block number)

The use of an impurity doped silicon MOSFET as an infrared detector (IRFET) has recently been proposed. This report gives a description of the operation of this new type of infrared detector and provides experimental verification of the design.

The IRFET is an integrating static read only memory element whose conductance is modulated by infrared radiation. Operation

over

DD FORM 1 JAN 73 1473 EDITION OF 1 NOV 65 IS OBSOLETE

Unclassified

SECURITY CLASSIFICATION OF THIS PAGE (When Data Entered)

409 489. mb

has been observed and characterized using the gold acceptor level and gold donor level in the near infrared wavelength range from 1.0 to 3.0 microns. It will be shown from pulsed capacitance measurements on MOS capacitors and from measurement of the IRFET response that the characteristics of the gold impurity center in the surface space charge region correspond to the results observed previously for the center in bulk silicon. Operation of the IRFET can then be described on the basis of a simple model where the change in charge state of the impurity center in the surface space charge region due to photoionization modulates the threshold voltage of the MOSFET and thus conductance of the device.

The IRFET has a very high gain and responsivities of 10 milliwatts/microjoule are easily achieved. Standard silicon MOSFET technology is employed and it should be possible to use other impurity centers to extend the response out to a wavelength of 14 microns. Applications in large scale integrated infrared imaging and target tracking arrays are anticipated.

TECHNICAL REPORT SUMMARY

Gold doped metal-oxide-silicon field effect transistors (MOSFET's) were fabricated and the infrared response characteristics of these devices experimentally determined in the near infrared wavelength range from 1.0 to 3.0 micrometers (microns). The objective of this work has been to verify operation of this new type of infrared detector and demonstrate some of the very unique characteristics. Extensions of this work to other impurity centers in silicon will follow naturally from this work in order to achieve infrared response in the middle and far infrared regions.

It has been demonstrated that this new type of detector works in the manner originally anticipated and according to the design calculations and criteria which have been previously published in the IEEE Trans. on Electron Devices Aug. 1974, pp 459-462. This new type of infrared detector, which has been assigned the acronym IRFET, is a static or D.C. read only memory element whose conductance is modulated by infrared radiation. The IRFET is an integrating detector suitable for use in imaging or target tracking arrays, and is based upon relatively well known silicon technology. The IRFET has been demonstrated to have very unique characteristics and no other infrared detector works in exactly the same manner, which makes a comparison with other types of detectors difficult. On the other hand, very high responsivities of the order 10 milliwatts/microjoule are easily achieved with the gold doped devices.

Work is currently in progress to characterize indium doped silicon devices in the 3 to 5 micrometer (micron) range and later work under this contract calls for the characterization of gallium doped devices in the 8 to 14 micrometer range.

Consideration is also being given to the best technique of application of these devices and since they are based on silicon technology where large scale integrated arrays are routinely fabricated it might not be unreasonable to anticipate that such IRFET detectors might not be available to be employed in some particular DoD application in the relatively short term future.

TABLE OF CONTENTS

INFRARED RESPONSE OF IMPURITY DOPED SILICON MOSFET's:
Experimental Characterization of the Infrared Response
of Gold Doped Silicon MOSFET's (IRFET's)

INTRODUCTION

The use of extrinsic, or impurity doped silicon MOSFET's, has been recently proposed for the fabrication of infrared imaging and target tracking arrays.(1,2) This report describes the initial work which has been done to verify operation of this new type of device and demonstrate the design characteristics and equations by using the specific example of a gold-doped device.

Gold-doped devices were chosen for this demonstration not only because they might be useful in the near infrared region but also because considerable information is available on the characteristics of gold in silicon and these devices would thus be the easiest to fabricate and characterize.

During initial phases of the work some time was required not only to set-up the fabrication and measurement equipment but also to establish the gold diffusion process for doping the devices. In this latter respect, it was decided to employ gold-doped MOS capacitors to determine the gold concentration in the diffused wafers and to determine the thermal and optical characteristics of the gold impurity center in surface space charge or depletion regions. Once the MOS capacitors were characterized then it was a relatively easy step to fabricate and characterize the MOS transistor or MOSFET. Although the contract only called explicity for a characterization of the response employing the gold donor level, results have been also obtained for the gold acceptor level in order to cover the more general case and the entire near infrared range.

EXPERIMENTAL RESULTS - MOS CAPACITOR

Gold-doped MOS capacitors, as shown in Fig. 1, were fabricated and a gated metal guard ring employed to avoid any possible problem with surface inversion and leakage. These devices were fabricated using standard silicon MOS techniques,

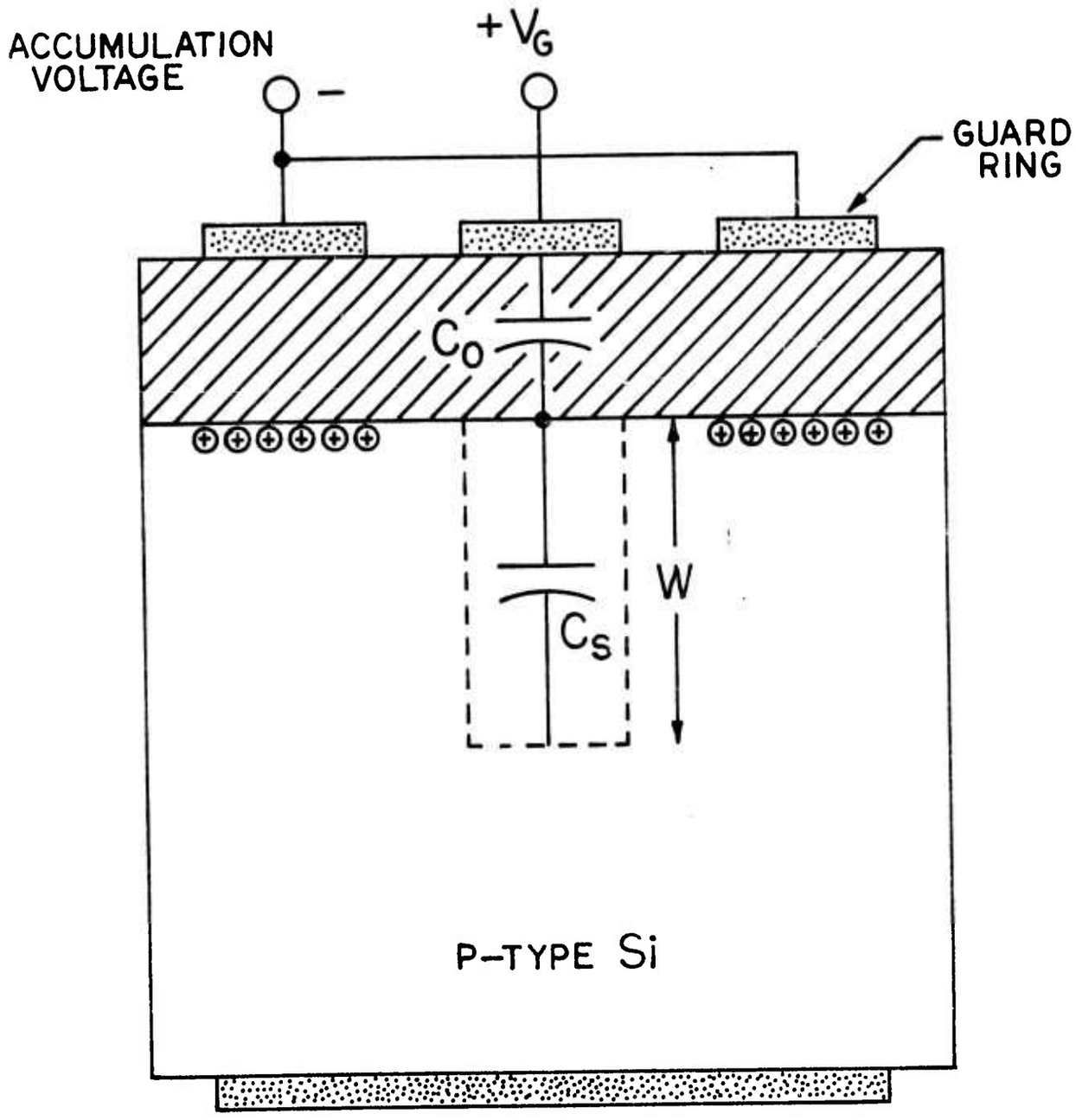

Fig. 1. Gold-Doped MOS Capacitor with Guard Ring

and the surface under the guard ring accumulated by applying a negative gate potential. The characteristics of the center MOS capacitor were measured by mounting the device in a temperature controlled sample chamber and determining the Capacitance-Voltage (C-V) or time dependence of the pulsed bias capacitance (C-t) transients.

Gold is a double-level impurity in silicon, as shown in Fig. 2, by the Shockley-Read-Hall model. (3) In a surface depletion region, or space charge region, however one need only be concerned with the emission processes in the S.R.H. model, which are either thermal or optical emission. At low temperatures the thermal emission rate is very small and the gold center will remain in a fixed charge state in a depletion region. (4,5,6,7)

Figure 3 shows the type of C-V curves observed on a MOS capacitor diffused with gold at 1000°C for 20 minutes. The accumulation capacitance is obtained for negative gate voltages, while for positive gate voltage three distinctly different characteristics are exhibited. The "normal" inversion capacitance can be observed by illuminating the sample with white light to generate sufficient minority carriers or electrons to form the inversion layer. At low temperatures the thermal generation rate of minority carriers is very low. More interesting however are the depletion characteristics which are relatively easy to observe and there are two distinctly different curves depending on whether the gold centers are in the positive or neutral charge state in the surface depletion region. (8,9)

The lower curve corresponds to the case where the gold is in the positive charge state which is observed by accumulating the surface, or drawing holes to the surface with a negative gate potential, and then applying an increasing positive potential. Following this the gold centers are either allowed to emit holes thermally from the donor level to valence band, or the sample is illuminated with infrared radiation to cause hole emission. The upper depletion curve is observed following the transient associated with hole emission when all the gold

GOLD IMPURITY CENTER IN SILICON

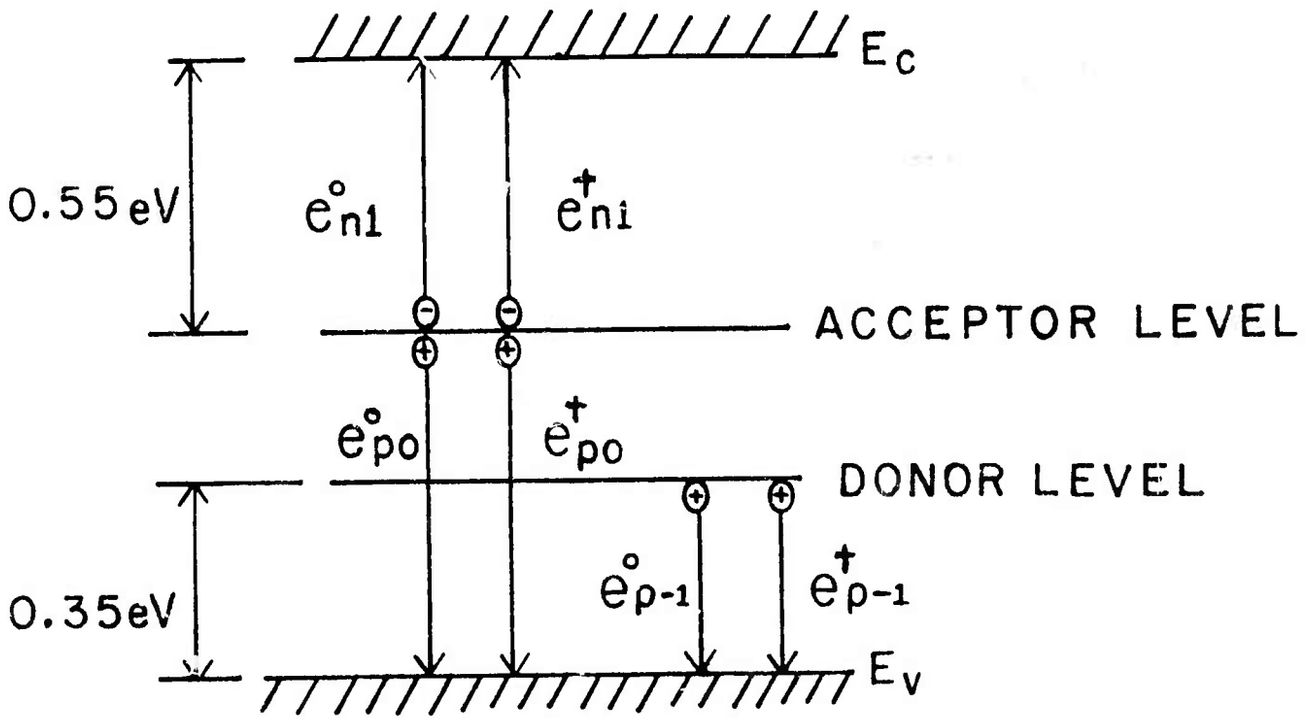

Fig. 2. Cold in Silicon and the Important Emission Processes

is in the neutral charge state. The gold concentration can be accurately determined from the depletion curves and the optical or thermal emission rates determined from the transient decay.

The depletion capacitance is the series combination of the oxide capacitance, C_o, and the semiconductor capacitance, C_s. The dependence of the semiconductor capacitance upon the amount of gate voltage in excess of that to first cause depletion, the depletion voltage, can be calculated by employing Poisson's equation and matching the electric field at the surface of the semiconductor and the electric field in the oxide. In this manner it can be shown in a relatively straightforward calculation that the depletion capacitance of the MOS capacitor is given by: (8,9)

$$C_{HF} = \frac{K_o \varepsilon_o A}{X_o} \cdot \frac{1}{\sqrt{1 + \left(\frac{K_o}{K_s}\right)^2 \frac{1}{X_o^2} \left(\frac{2K_s \varepsilon_o V}{q N_I}\right)}}$$

where

q = Electron charge (coulombs)

X_o = Oxide thickness (cm)

ε_o = Electric permittivity free space (F/cm)

K_o = Dielectric constant of oxide

K_s = Dielectric constant of silicon

A = Area (cm^2)

V = Depletion voltage (Volts)

N_I = Ionized impurity center concentration ($1/cm^3$)

If the gold is in the neutral charges state then $N_I = N_A$, where N_A is the substrate doping of shallow level boron or shallow level acceptor concentration. If the gold is in the positive charge state then $N_I = N_A - N_{TT}$, where N_{TT} is the gold concentration.

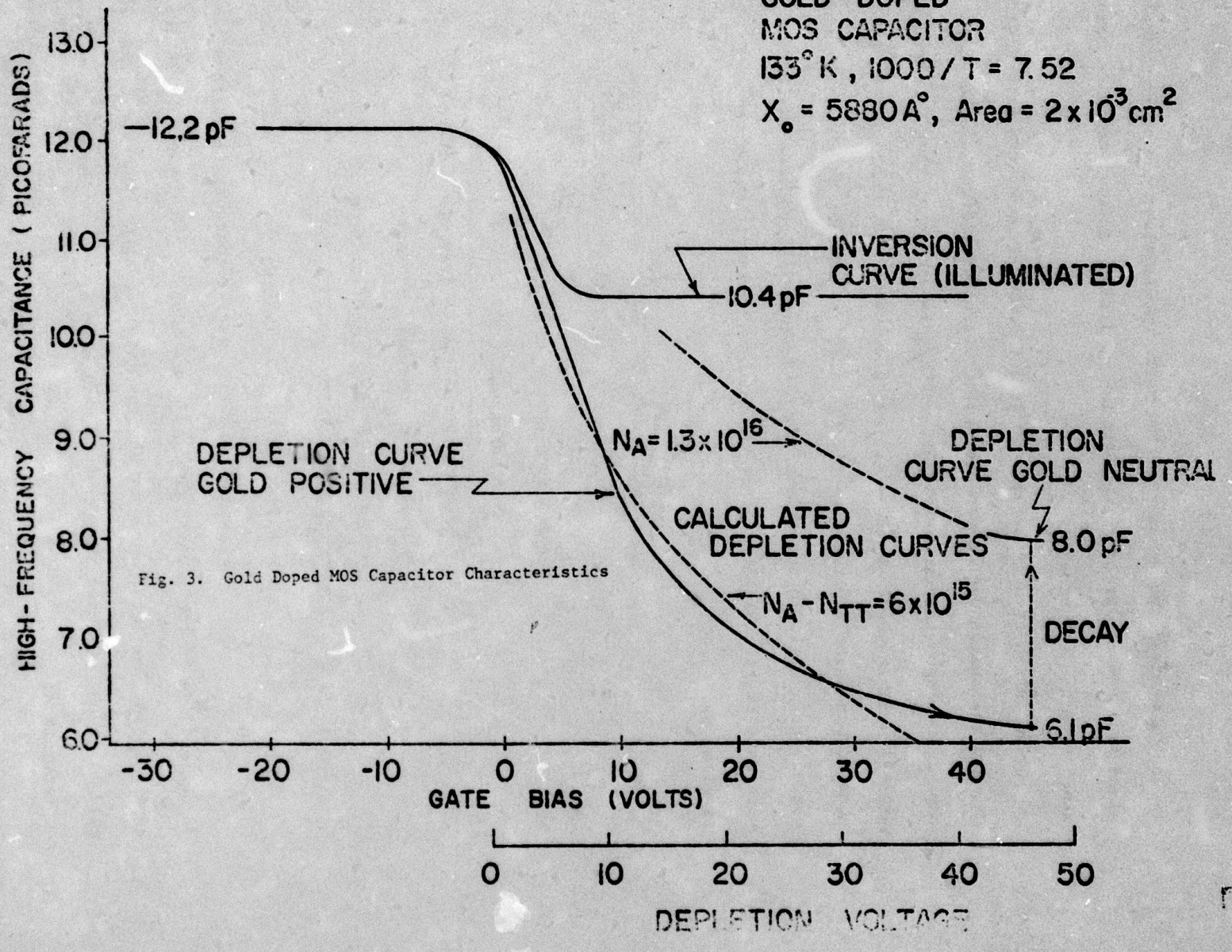

Fig. 3. Gold Doped MOS Capacitor Characteristics

Numerical calculations have been performed and matched to the C-V curves in Figure 3. These yield a gold concentration of $N_{TT} = 5X10^{15}/cm^3$ for a 1000°C 20 min gold diffusion and an acceptor or boron wafer doping of $N_A = 1.3X10^{16}/cm^3$ for the nominal 1 ohm-cm wafer.

The time dependence of the transient between the two depletion curves can be obtained from Equation(1)by using $N_I = N_A - P_T(t)$ where $P_T(t)$ is the time dependence of the gold in the positive charge state. By defining

$$-\Delta C_{HF}(t) = C_{HF}(t) - C^f_{HF}(N_I=N_A) \tag{2}$$

and then using a binomial expansion in Equation(1)one obtains

$$\Delta C_{HF}(t)/C_o = \frac{1}{2}\ \frac{b}{N_A}\ \frac{1}{\left(1+\frac{b}{N_A}\right)^{3/2}}\ \frac{P_T(t)}{N_A} \tag{3}$$

where

$$C_o = K_o \varepsilon_o A/X_o \tag{4}$$

and

$$b = \left(\frac{K_o}{K_s}\right)^2\ \left(\frac{1}{X_o^2}\right)\ \left(\frac{2K_s\varepsilon_o V}{q}\right) \tag{5}$$

The time dependence of the gold charge state is determined by the capture and emission rates in the S. R. H. model and is given by: (3,4)

$$\frac{dP_T}{dt} = -C_n\ n\ P_T + C_p p\ N_T + e_n\ N_T - e_p\ P_T \tag{6}$$

in a depletion region, n=p= 0, and for the gold donor level $e_p >> e_n$ since the level is closer to the valence band edge. Then, for the gold donor level, equation (6) becomes

$$\frac{dP_T}{dt} = -e_p\ P_T \tag{7}$$

The initial condition is determined by accumulating the surface at time t=0 and insuring all the gold starts in the positive charge state. The solution is

$$P_T(t) = N_{TT}\ e^{-t/\tau} \tag{8}$$

where

$$\tau = \frac{1}{e_p} = \frac{1}{e_{p-1}} \tag{9}$$

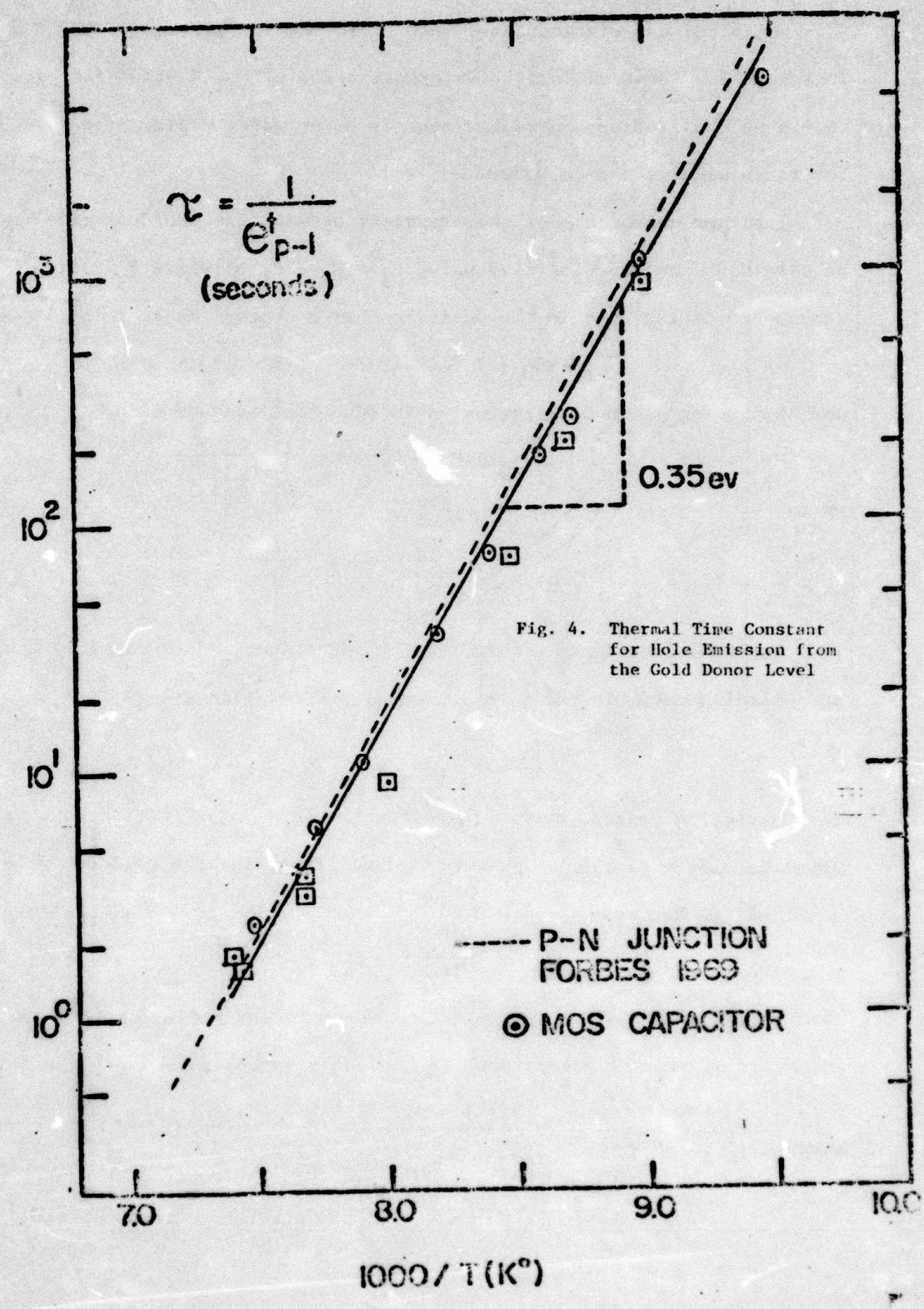

Fig. 4. Thermal Time Constant for Hole Emission from the Gold Donor Level

The designation e_{p-1} indicates that the hole emission occurs from gold centers in the positive charge state, and in addition, this emission may be due to thermal and/or optical emission. If one measures the time constant of the capacitance transient associated with thermal emission as a function of temperature one can thus determine the thermal emission rate. This has been done and is shown in Figure 4. The thermal emission rate is of the form,

$$e_{p-1} = A\, e^{-\Delta E/kT} \quad \text{or} \quad \tau = (1/A)\, e^{\Delta E/kT} \tag{10}$$

so that the slope of the line in Figure 4 determines the energy difference ΔE which in this case is 0.35 eV. The results are also shown to correspond closely to the results obtained previously by the author for the donor level of gold in bulk silicon by measuring transients on p-n junctions. Thus there can be little doubt that the gold impurity center is being observed and the 1000°C, 20 min diffusion cycle introduces a convenient concentration of gold into the MOS surface depletion region.

Optical emission can also be observed if the temperature is low enough such that $e^{o}_{p-1} >> e^{t}_{p-1}$. Then $e^{o}_{p-1} = \sigma^{o}_{p-1}(\hbar w) \cdot \Phi$ where $\sigma^{o}_{p-1}(\hbar w)$ is the photoionization cross section and Φ the photon flux, (#/cm^2 . sec). These measurements were also performed to verify that the center has a threshold ionization energy of 0.35 eV. These results are, however, not shown since this subject will be treated more thoroughly in describing the characterization of the infrared sensing MOSFET.

EXPERIMENTAL RESULTS - MOS TRANSISTOR

The operation of the MOS transistor, or MOSFET, which is shown in Figure 5 follows directly from the previous discussion. In the case of the infrared sensing MOSFET or IRFET, however, the modulation of the space charge in the depletion region results in a change of threshold voltage and conductance of the device.

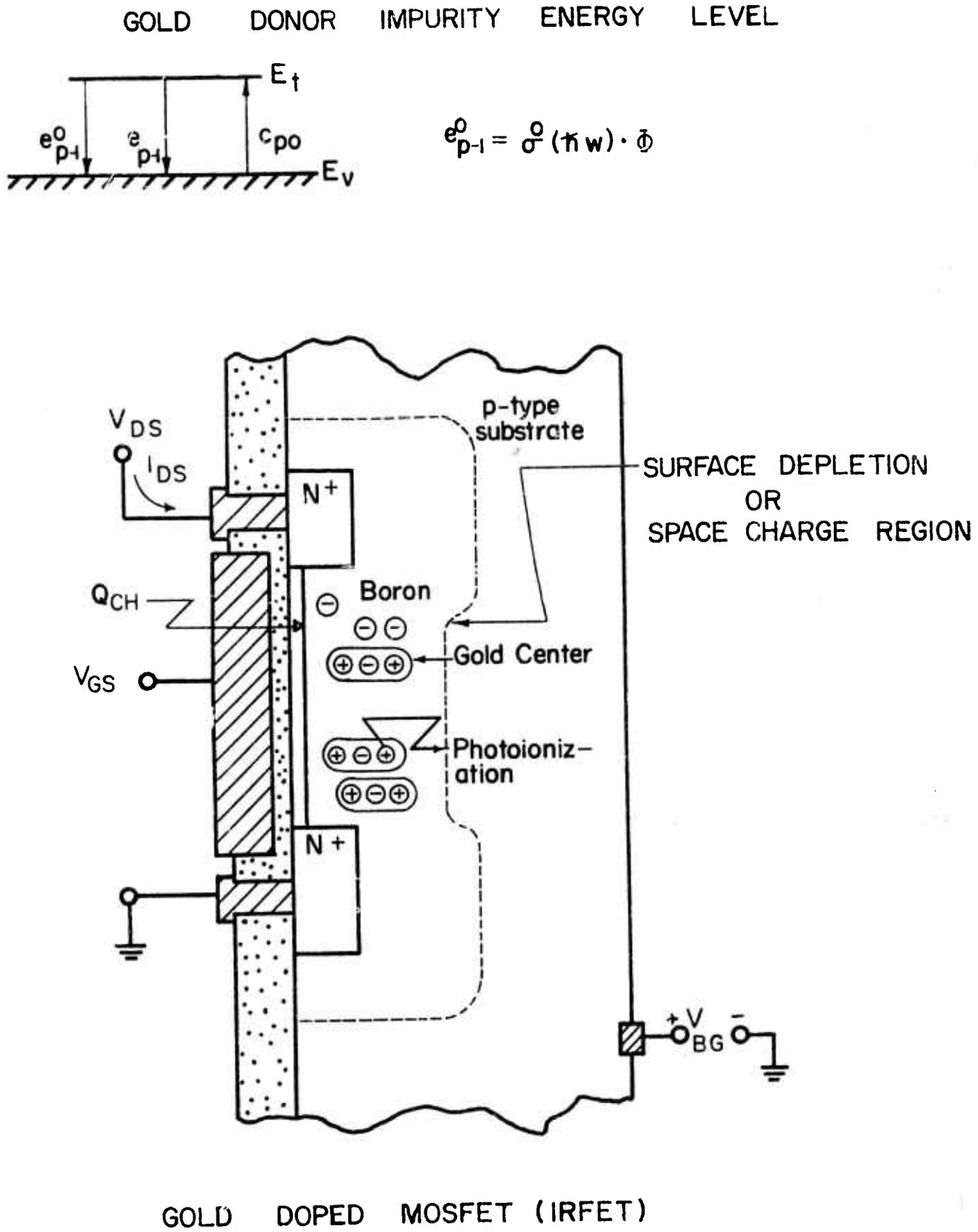

Fig. 5. The Infrared Sensing MOSFET (IRFET) Device Structure

The threshold voltage of a MOSFET such as that shown in Figure 5 can be written as,(10)

$$V_T=(\phi_{ms} - Q_o/C_o + 2|\phi_f|) +(X_o K_s/K_o)\sqrt{\frac{2(2|\phi_f| + |V_{BG}|)\ q\ N_I}{K_s \varepsilon_o}} \quad (11)$$

where

ϕ_{ms} = metal-semiconductor work function difference

ϕ_f = Fermi potential in the bulk semiconductor

Q_o = equivalent or effective oxide charge

V_{BG} = Back gate or substrate bias

As before N_I, the ionized impurity concentration, in the surface space charge region depends on the gold charge state and specifically for the gold donor level response,

$$N_I = N_A - P_T \quad (12)$$

$$P_T = N_{TT}\, e^{-t/\tau} \quad (13)$$

$$\tau = 1/e_p = 1/e_{p-1} \quad (14)$$

If the change in threshold voltage ΔV_T is defined as

$$\Delta V_T = V_T^f - V_T^i \quad (15)$$

then

$$\Delta V_T =(X_o\ K_s/K_o)\cdot\sqrt{\frac{2(2|\phi_f| + |V_{BG}|)\ q\ N_A}{K_s \varepsilon_o}}\cdot\left(\frac{N_{TT}}{2N_A}\right) \quad (16)$$

ΔV_T is the total change in threshold voltage between the cases where the gold charge state is positive and neutral.

The method of operation of the IRFET is to first accumulate the surface and fill the gold centers with holes. The normal inverting or more positive gate voltage is then applied which will result in conduction between the source and drain. The gold centers in the surface depletion or space charge region can then either thermally or optically emit a hole to the valence band.

The change in threshold voltage ΔV_T will result in a change in conductance which can be described by the simple equations describing the drain current I_{DS}(10).

STATIC D.C. CHARACTERISTICS

LINEAR REGION $-V_{DS} < V_{GS} - V_T$

$$I_{DS} = (\mu C_O)\cdot(W/L)\cdot(V_{GS} - V_T - V_{DS}/2)V_{DS}$$

SATURATION REGION $V_{DS} > V_{GS} - V_T$

$$I_{DS} = (\mu C_O)\cdot(W/L)\cdot\left(\frac{(V_{GS} - V_T)^2}{2}\right)$$

CHANGE DUE TO ILLUMINATION

$$\Delta V_T = V_T^f - V_T^i \qquad \Delta I_{DS} = I_{DS}^f - I_{DS}^i$$

LINEAR REGION $V_{DS} \leq V_{GS} - V_T^i - \Delta V_T$

$$-\Delta I_{DS} = (\mu C_O)\cdot(W/L)\,\Delta V_T\, V_{DS}$$

INTERMEDIATE $V_{GS} - V_T^i - \Delta V_T \leq V_{DS} \leq V_{GS} - V_T^i$

$$-\Delta I_{DS} = (\mu C_O)(W/L)\Big[(V_{GS} - V_T^i - \Delta V_T/2)\,\Delta V_T + (V_{GS} - V_T^i)V_{DS} + V_{GS}V_T^i - (V_{GS}^2/2 + V_T^{i2}/2 + V_{DS}^2/2)\Big]$$

SATURATION REGION $V_{DS} \geq V_{GS} - V_T^i$

$$-\Delta I_{DS} = (\mu C_O)(W/L)(\Delta V_T)(V_{GS} - V_T^i - \Delta V_T/2)$$

Fig. 6. Equations for MOSFET (IRFET) Operation

These equations have been summarized in Figure 6, where:

ΔI_{DS} = total change in drain current in response to ΔV_T

μ = effective electron surface mobility

V_{DS} = drain to source voltage

V_{GS} = gate to source voltage

and W/L = width to length ratio of the channel.

Figure 7 shows the experimentally measured characteristics for the total, or maximum, change in drain current ΔI_{DS} using the response from the gold donor level on a particular device. Figures 8 and 9 show a detailed investigation of both the response in the linear region and the saturation region of operation.

In the linear region of operation $V_{DS} < V_{GS} - V_T^i - \Delta V_T$ and the simple analysis predicts

$$\Delta I_{DS} = -\mu C_o (W/L) \Delta V_T \cdot V_{DS} \quad (17)$$

while in the saturation region $V_{DS} > V_{GS} - V_T^i$

and

$$\Delta I_{DS} = -\mu C_o (W/L)(\Delta V_T)(V_{GS} - V_T^i - \Delta V_T/2) \quad (18)$$

Figures 8 and 9 show that the observed characteristics closely follow these functional forms, except near threshold which is expected and deviate only slightly at high gate voltage due to the field dependent surface mobility.

Equations (11) and (16) also show that the threshold voltage, V_T, and maximum or total change in threshold voltage ΔV_T are functions of the substrate or back-gate bias. Figure 10 shows the experimentally observed dependence of the initial threshold voltage, V_T^i, and final threshold voltage V_T^f, on back gate bias. Using equation (11) then the substrate doping concentration and gold doping concentrations can be calculated, yielding values of $N_A = 1.0 \times 10^{16}/cm^3$ and $N_{TT} = 2 \times 10^{15}/cm^3$. In this case the gold concentration is slightly lower than for the MOS capacitor shown previously since the diffusion cycle was 1000^oC for 7 minutes rather than 20 minutes.

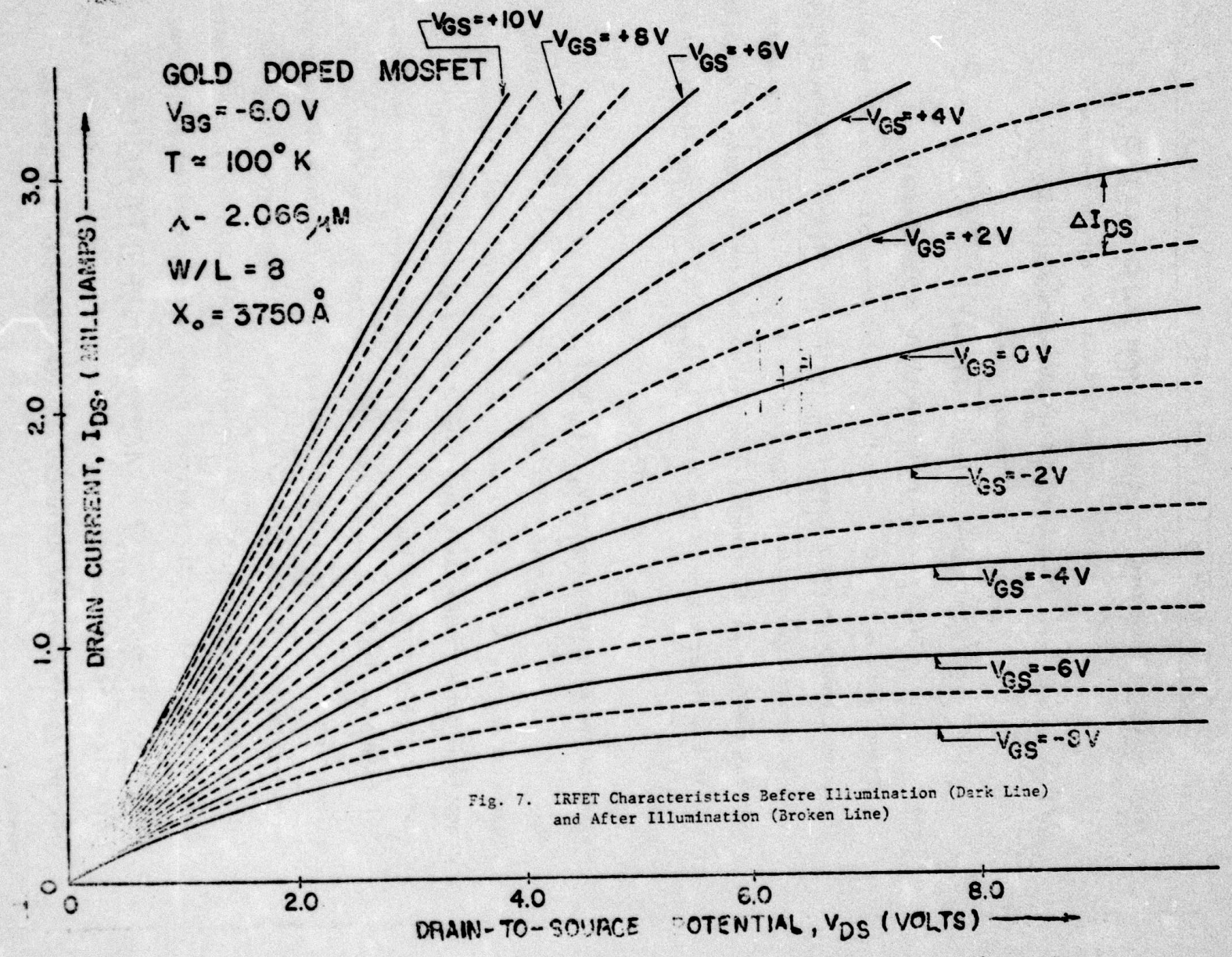

Fig. 7. IRFET Characteristics Before Illumination (Dark Line) and After Illumination (Broken Line)

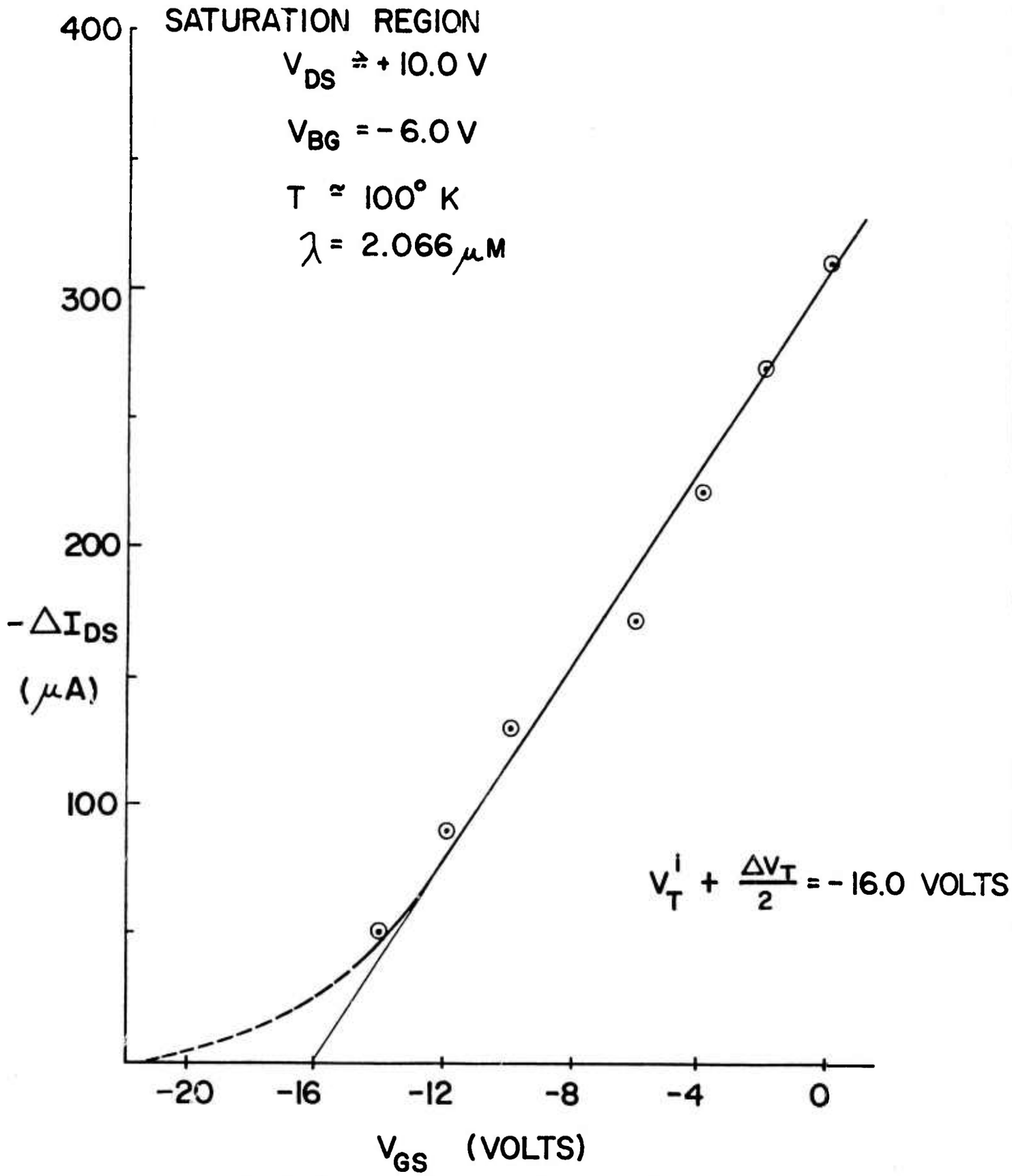

Fig.8. Change in I_{DS} in the Saturation Region

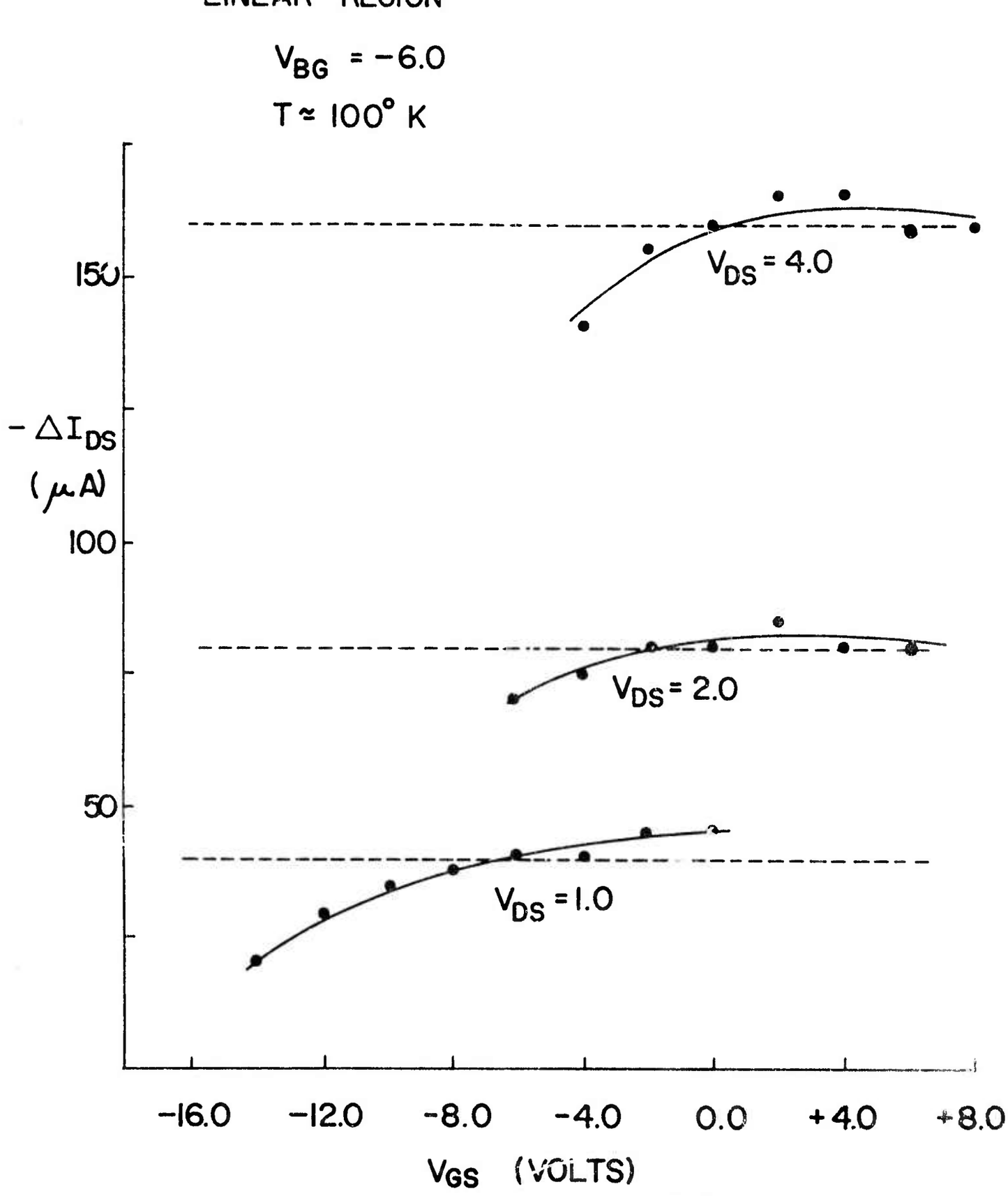

Fig. 9. Change in I_{DS} in the Linear Region

The threshold voltage in Figure 10 has been obtained by exptrapolating the linear region characteristics back to $I_{DS} = 0$.

In calculating the substrate doping and gold doping an oxide thickness of 3750 A^{o} has been employed which corresponds to the gate oxidation process and color which give a thickness of less than the order 4000 A^{o}. The particular device shown in Figure 7 has a W/L ratio of 8 and a channel length L of 7.0 mils.

The equations for the static or D. C. current, given in Figure 6, in the saturation region and linear region can be used to calculate the effective surface mobility, μ, at the temperature of operation, $100^{o}K$. These yield values of

$$\mu \text{ (linear region)} = 350 \text{ cm}^2/\text{V. sec for } V_{GS} = 4V, \; V_{DS} = 7V$$

$$\mu \text{ (saturation region)} = 246 \text{ cm}^2/\text{V. sec for } V_{GS} = -12V$$

Gold doping has been found to reduce the effective surface mobility in surface channel devices presumably due to excess scattering due to interface or oxide charge introduced by the gold.

The characteristics for the change in drain to source current, ΔI_{DS}, as described by equations (17) and (18) can be compared to the equations in Figure 6 for the total drain to source current, I_{DS}, to yield;

$$\Delta V_T \text{ (linear region)} = \frac{-\Delta I_{DS} \; (V_{GS} - V_T^i - V_{DS/2})}{I_{DS}^i}$$

and

$$\Delta V_T \text{ (saturation region)} = \frac{-\Delta I_{DS} \; (V_{GS} - V_T^i)}{2 \; I_{DS}^i}$$

if

$\Delta V_T << V_{GS} - V_T^i$ in the saturation region

These yield values of ΔV_T (linear region)=1.67 Volts and ΔV_T (saturation region)=1.10 Volts.

Both a lower value of mobility and a smaller change in threshold voltage, ΔV_T, are required to match the characteristics in the saturation region as compared to the linear region, presumably this is due to the field dependence of the mobility which has not been included in the original model and equations in Figure 6.

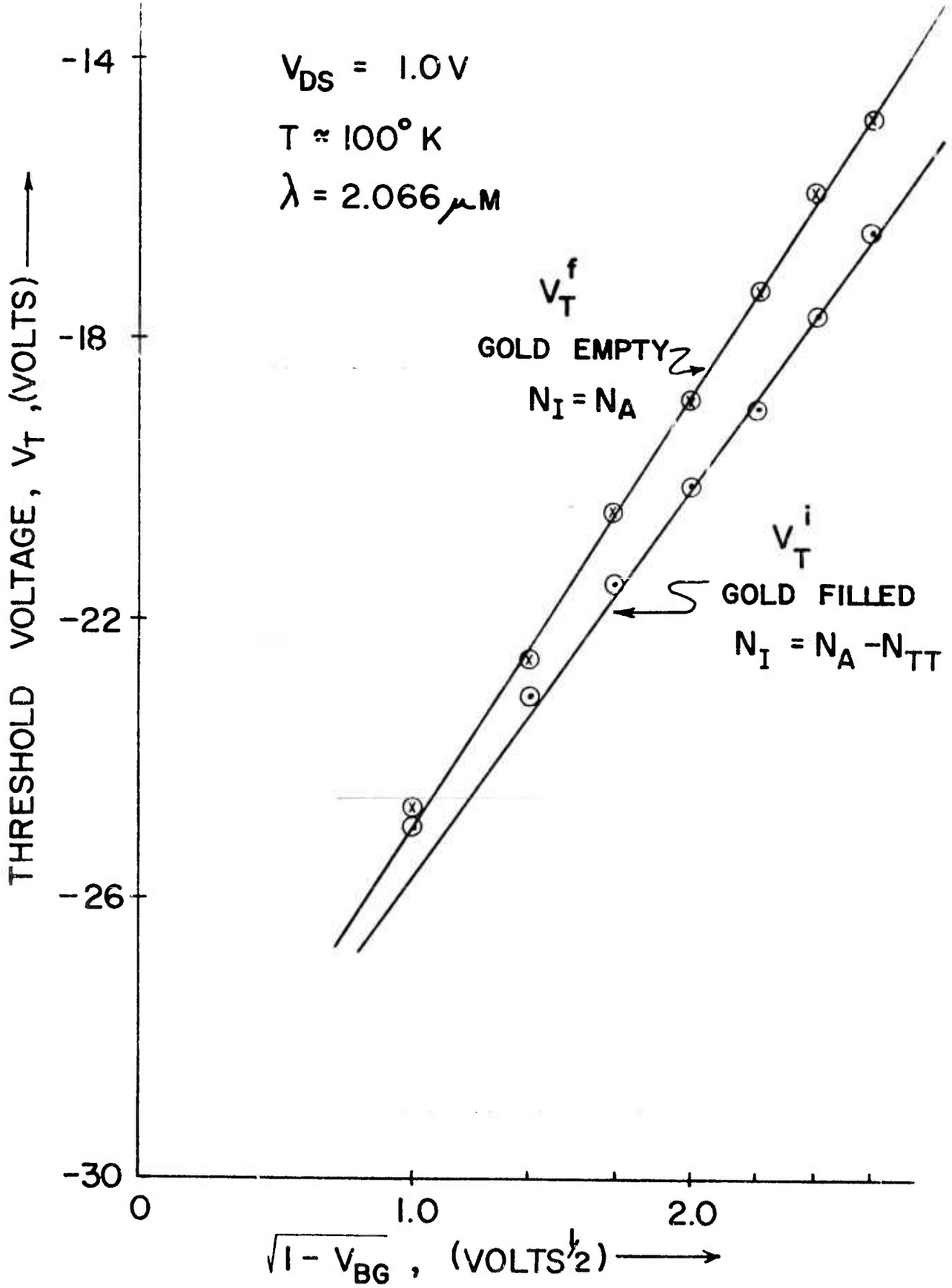

Fig. 10. Dependence of Threshold Voltage on Back Gate Bias

When operating the IRFET as an infrared detector one is of course more concerned with the transient response, than the steady-state limits of operation, where the gold in entirely one charge state or another. The time dependence of the charge in threshold voltage $\Delta V_T(t)$ can be written as,

$$\Delta V_T(t) = X_o(K_s/K_o)\sqrt{\frac{((2|\phi_f| + |V_{BG}|)\ q\ N_A)}{K_s \varepsilon_o}} \cdot \left(\frac{N_{TT}}{2N_A}\right)(1-e^{-t/\tau}) \quad (19)$$

where, as before, $\tau = 1/e_p$ and for the donor level, $e_p = e_{p-1}$. There will then be a time dependent transient change in the current given in the linear region by

$$-\Delta I_{DS}(t) = (\mu C_o)\ (W/L)\ V_{DS}\ \Delta V_T\ (t) \quad (20)$$

and in the saturation region by

$$-\Delta I_{DS}(t) = (\mu C_o)\ (W/L)\ (V_{GS} - V_T^{\,i})\ \Delta V_T(t) \quad (21)$$

These transients can be conveniently observed by mounting the sample in a temperature controlled sample chamber which has provision for illumination of the sample and which has been illustrated in Figure 11. The time constant of the thermal decay determined as the temperature is varied can be employed to determine the thermal emission rate. Figure 12 shows the time dependence of the thermal decay as a function of temperature. It is seen that the results correspond very closely to those obtained previously for the gold donor level using the MOS capacitor and p-n junction techniques. There can be little doubt that this response is due to the gold donor level and on the basis of Figures 7,8,9, and 10 that the characteristics of the device can be described on the basis of a modulation of space charge in the surface depletion region.

When operating the device as an infrared detector, the idea would of course be to use a low enough temperature so that thermal emission is negligible. In the case of the donor level then the emission can only be due to optical emission and $e_{p-1} = e^{o}_{p-1}$.

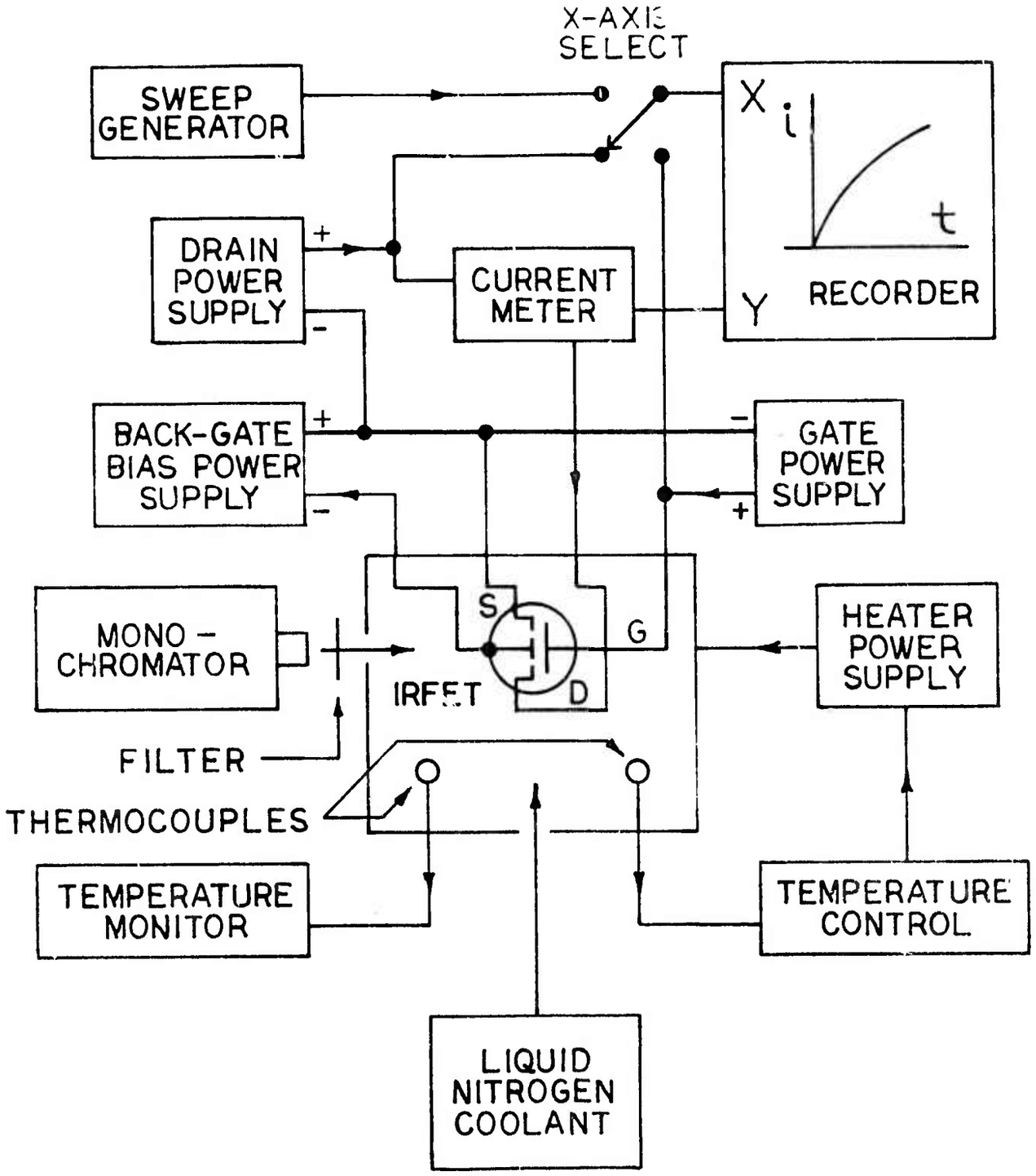

Fig. 11. Temperature Controlled Sample Chamber and Measurement Technique

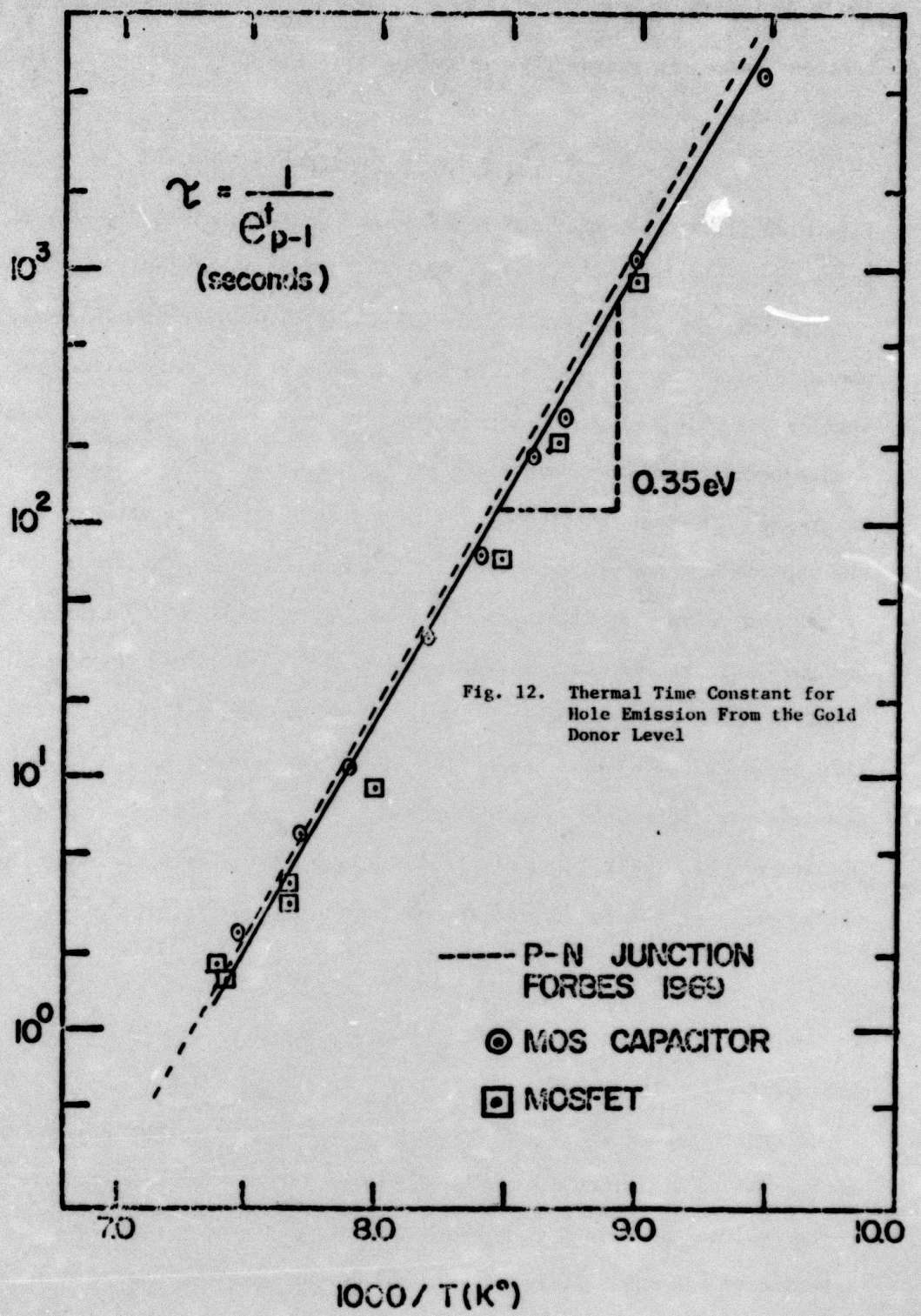

Fig. 12. Thermal Time Constant for Hole Emission From the Gold Donor Level

Where as before $e_{p-1} = \sigma^{o}_{p-1}(\hbar w) \cdot \Phi$; σ^{o}_{p-1}, (cm^2), is the photoionization cross section, and Φ the photon flux (#/cm^2. sec). The time constant of the current decay is then,

$$\tau = 1/e^{o}_{p-1} = 1/(\sigma^{o}_{p-1}(\hbar w) \cdot \Phi) \quad . \tag{22}$$

Figure 13 illustrates the time constant associated with the current decay for a particular device and bias and illumination conditions.

The response of the IRFET to infrared radiation is thus determined by the photoionization cross section, in this example by the photoionization cross section for hole emission from the donor level. However, because gold is a double level impurity response can also be observed for the acceptor level in the range of photon energies 0.6 eV to 1.1 eV. Figure 14 shows first of all the photoionization cross section for the donor level, σ^{o}_{p-1}, as a function of the photon energy, $\hbar w$, in the range 0.375 eV to 0.7 eV. At higher photon energies and/or temperatures response can also be observed for the acceptor level. In the case of acceptor level, first suppose all the gold is neutral, this can be arranged by illumination in the range where σ^{o}_{p-1} is large or by operation at higher temperatures where e^{t}_{p-1} is large, but low enough such that e^{t}_{po} and e^{t}_{n1} are small. The time constant associated with the neutral-negative charge state transition is then by analogy with equation (6) given by

$$\tau = 1/(e^{o}_{p} + e^{o}_{n1}) = 1/\Phi \cdot (\sigma^{o}_{po} + \sigma^{o}_{n1}) \tag{23}$$

In the case of the acceptor level, however, which is near the center of the band gap it cannot be assumed either e^{o}_{po} or e^{o}_{n1} is small.

Figure 14 shows σ^{o}_{p-1}, and the sum σ^{o}_{po} and σ^{o}_{n1} as a function of photon energy which determines the response of the IRFET. The results have been corrected for the relative spectral dependence of the photon flux, Φ, but our experiments are not calibrated in terms of the absolute photon flux, Φ. Also

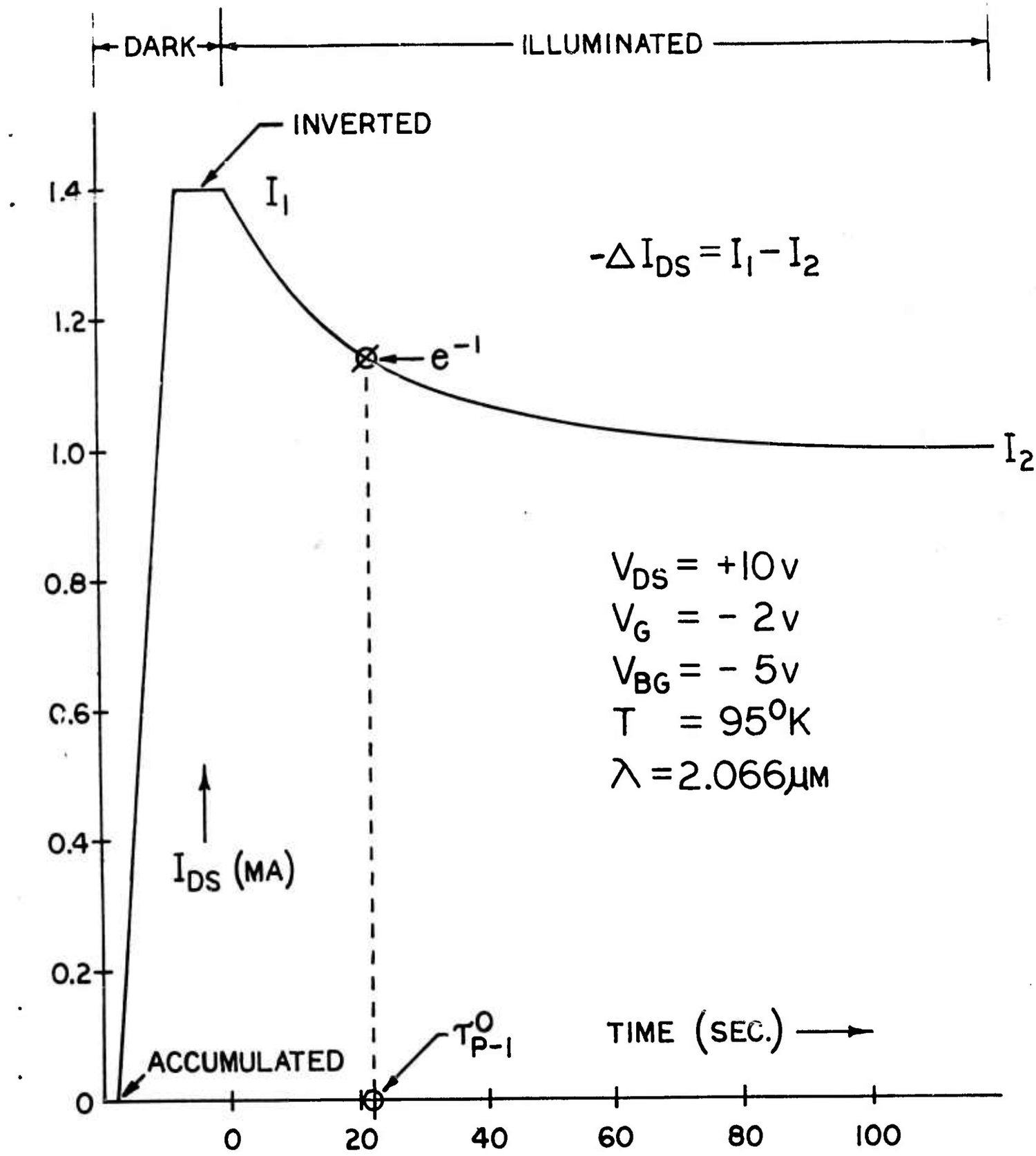

Fig. 13. Example of the Time Dependent Drain Current, I_{DS}, on the IRFET due to Illumination with Infrared Radiation

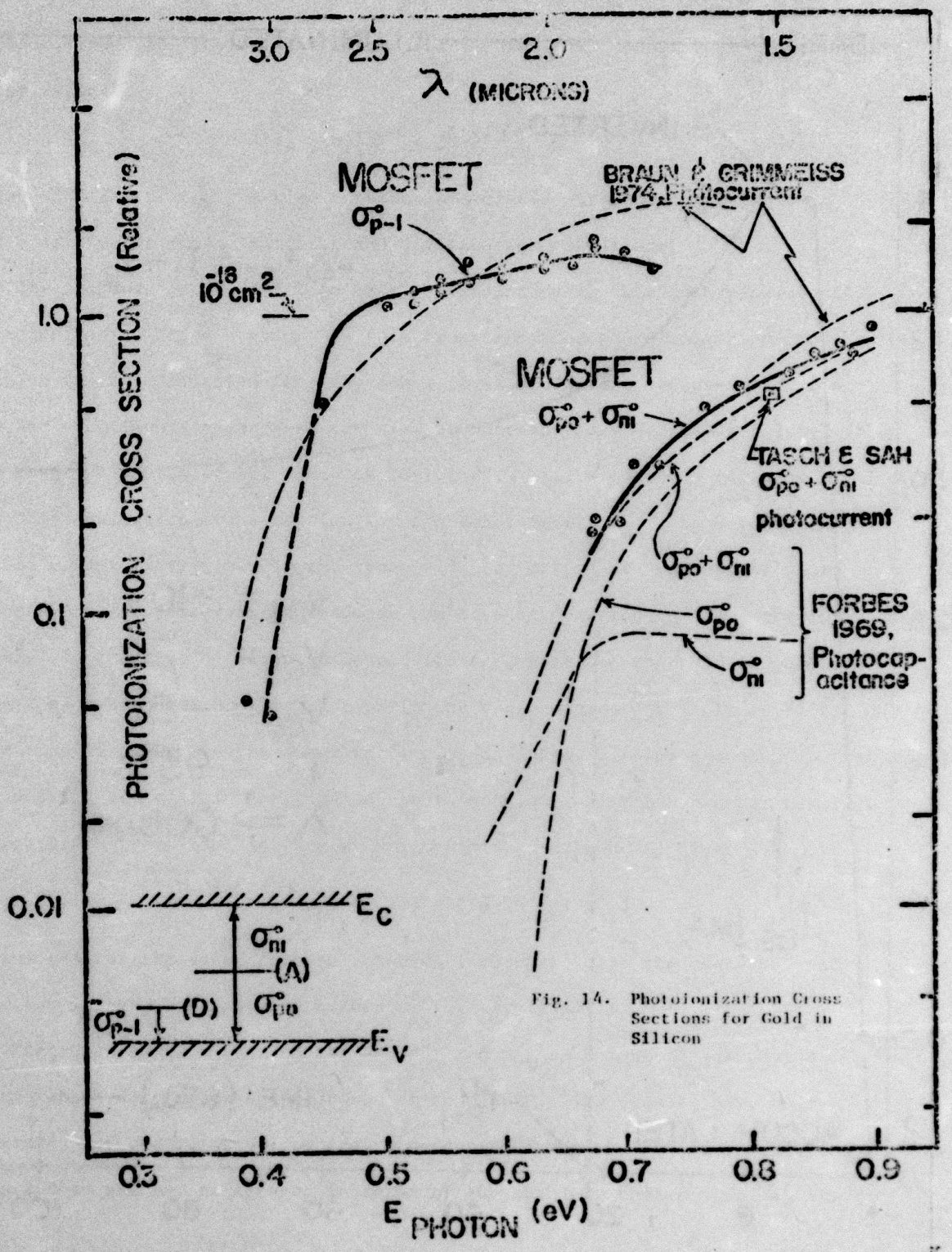

Fig. 14. Photoionization Cross Sections for Gold in Silicon

shown are the results previous obtained for gold in bulk silicon by the author (5), by Tasch and Sah (11), and more recently by Braun and Grimmeiss (12). In reality there is considerable difficulty in an absolute determination of the magnitude of the photoionization cross section due to reflections inside the device and large differences in very basic measurements between different laboratories in determining optical flux (13). The most likely calibration point, $10^{-16} cm^2$, has been indicated on Figure 14.

Knowing then the equations describing the device operation, and the temperature and photon energy dependence of the emission rates, one is in a position to be able to calculate the characteristics of the gold doped IRFET under any given set of circumstances. This information is sufficient to describe the important device characteristics.

FABRICATION CONSIDERATIONS

The gold doped MOS capacitors and transistors fabricated as part of this work are relatively simple devices, with in terms of integrated circuit devices relatively large areas. In the case of MOSFETs a three mask process has been employed with gate oxide thickness of around $4000A^{o}$ or less.

The gold doping has been achieved by evaporation of gold on the back of the wafer and subsequent diffusion at $1000^{o}C$ for times in the range 7 to 20 minutes. This produces gold concentrations in the active device areas of 2.0 to $5.0 \times 10^{15}/cm^3$ which are convenient doping levels. Individual devices have been mounted on TO5 headers for testing.

It has been found that gold doping the substrate appears to result in a net positive charge due to gold in the oxide and a threshold voltage shift to more negative voltages which is consistent with previous observations.(14). These n-channel MOSFET's are depletion mode or normally on devices and guard rings have been employed on MOS capacitors and circular or enclosed geometries for MOSFETs to avoid any possible effect on the results by surface inversion outside the active device area.

The only unusual feature noticed is that excess gold doping may in fact produce buried channel devices and/or abnormally large negative threshold voltages. The buried channel effect being noticed previously by a very high channel mobility, essentially the bulk mobility rather than the surface mobility. The exact reason for this buried channel effect with excess gold doping is not known.

Work is continuing on the gold doping process in conjunction with work aimed at checking on device uniformity and the fabrication of larger arrays of smaller devices. Part of this work will include the use of doped oxide sources to achieve gold doping, rather than the vacuum evaporation technique.

Obviously, in the case of slow diffusing impurities like indium and gallium it would be desireable to have these impurities introduced during crystal growth, it is in fact possible to have such work done on a special order basis from commercial firms.

IRFET RESPONSIVITY AND APPLICATIONS

The IRFET can either be operated in the linear or saturation region, however, for high responsivity and in order to make the characteristics independent of drain voltages, V_{DS}, it would seem most appropriate to operate it in the saturation region. In the saturation region, we have from equation (21),

$$-\Delta I_{DS}(t) = (\mu C_o)\ (W/L)\ (V_{GS} - V_T^i)\ \Delta V_T(t) \qquad (24)$$

where

$$\Delta V_T(t) = \Delta V_T(\max) \cdot (1-e^{-t/\tau}) \qquad (25)$$

If the time period, t, is much less than τ the time constant then,

$$1- e^{-t/\tau} \simeq 1-1 + t/\tau = t/\tau \qquad (26)$$

and there is a linear change in current, ΔI_{DS} , with time, where

$$-\Delta I_{DS}(t) = \Delta I_{DS}(\max).(t/\tau). \qquad (27)$$

If the IRFET integrates the incident optical signal for a period of time $t \ll \tau$ then there will be a total energy input of

$$E_{input} = \Phi \cdot t \cdot \hbar w \cdot A \qquad (28)$$

Where A is the active device area, $A = W \cdot L$. At the end of this integration

IRFET RESPONSIVITY

DONOR LEVEL

$T \lesssim 110^\circ K$

$W/L = 8$

AREA $= 2.5 \times 10^{-3}\ cm^2$

$X_o = 4000\ \text{Å}$

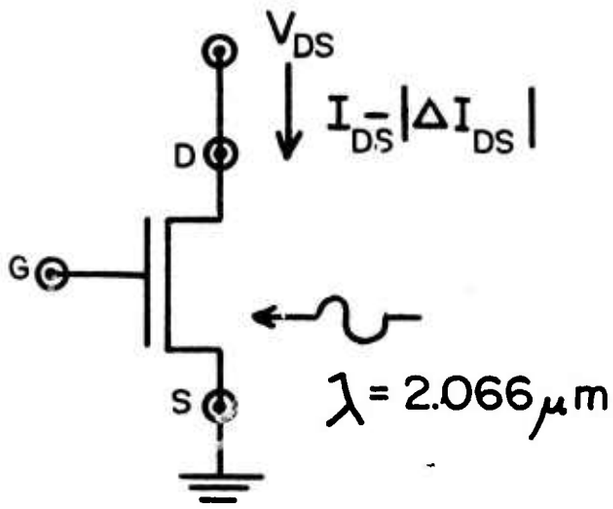

INPUT ENERGY

$\sigma^\circ = 1.5 \times 10^{-16}\ cm^2$

$\tau = 20$ sec., $\Phi = 3.3 \times 10^{-5}$ Watts/cm^2

$E_{in} = (t = \tau/10) = 1.67 \times 10^{-7}$ Joules

OUTPUT POWER, $t > \tau/10$

$|\Delta I_{DS}| \times V_{DS} = 0.1\ mA \times 16\ V$

$= 1.6$ milli Watts

$$\text{RESPONSIVITY} = \frac{\text{OUTPUT POWER}}{\text{INPUT ENERGY}}$$

$$= \frac{10 \text{ milli Watts}}{\text{micro Joule}}.$$

Fig. 15. An Example of Determination of the IRFET Responsivity

period, t, there will be a change in drain to source current by $-\Delta I_{DS}(t)$ and an output signal power of $\Delta I_{DS}(t) \cdot V_{DS}$. This output change is permanent until reset, and can be read for an indefinitely long period.

This has lead us to a definition of responsivity as

$$\text{RESPONSIVITY} = \frac{\text{SIGNAL POWER OUT}}{\text{SIGNAL INPUT ENERGY}} \qquad (29)$$

and an example is shown in Figure 15, where a responsivity of 10 milliwatts/microjoule is easily achieved using the donor level response.

Strangely enough the signal output power depends only on the W/L ratio of the device and not at all upon the device area, while, the signal input energy decreases directly with the area. Obviously even much higher responsivities might be achieved for small devices with the same W/L ratio, and in fact are limited only by the as yet undetermined noise limit.

The proposed method of application is to employ a large integrated array of IRFETs in infrared imaging and target tracking in conjunction with external auxiliary memory planes and electronic signal processing. If necessary three auxiliary memory planes might be employed to determine the time constant of the current decay associated with each element in the array. Since the time constant depends only on the flux and photionization cross section this should allow on accurate determination of the flux incident on each device in the array, and if necessary the detection of a small signal on a large background.

CONCLUSIONS AND FUTURE EXTENSIONS

The IRFET has been demonstrated to work according to the previously published design calculations and criteria. The IRFET is a very unique type of detector with some very unique characteristics some of which are summarized below. It is;

(i) a static read only memory element

(ii) an integrating detector

(iii) a negative photoconductivity element

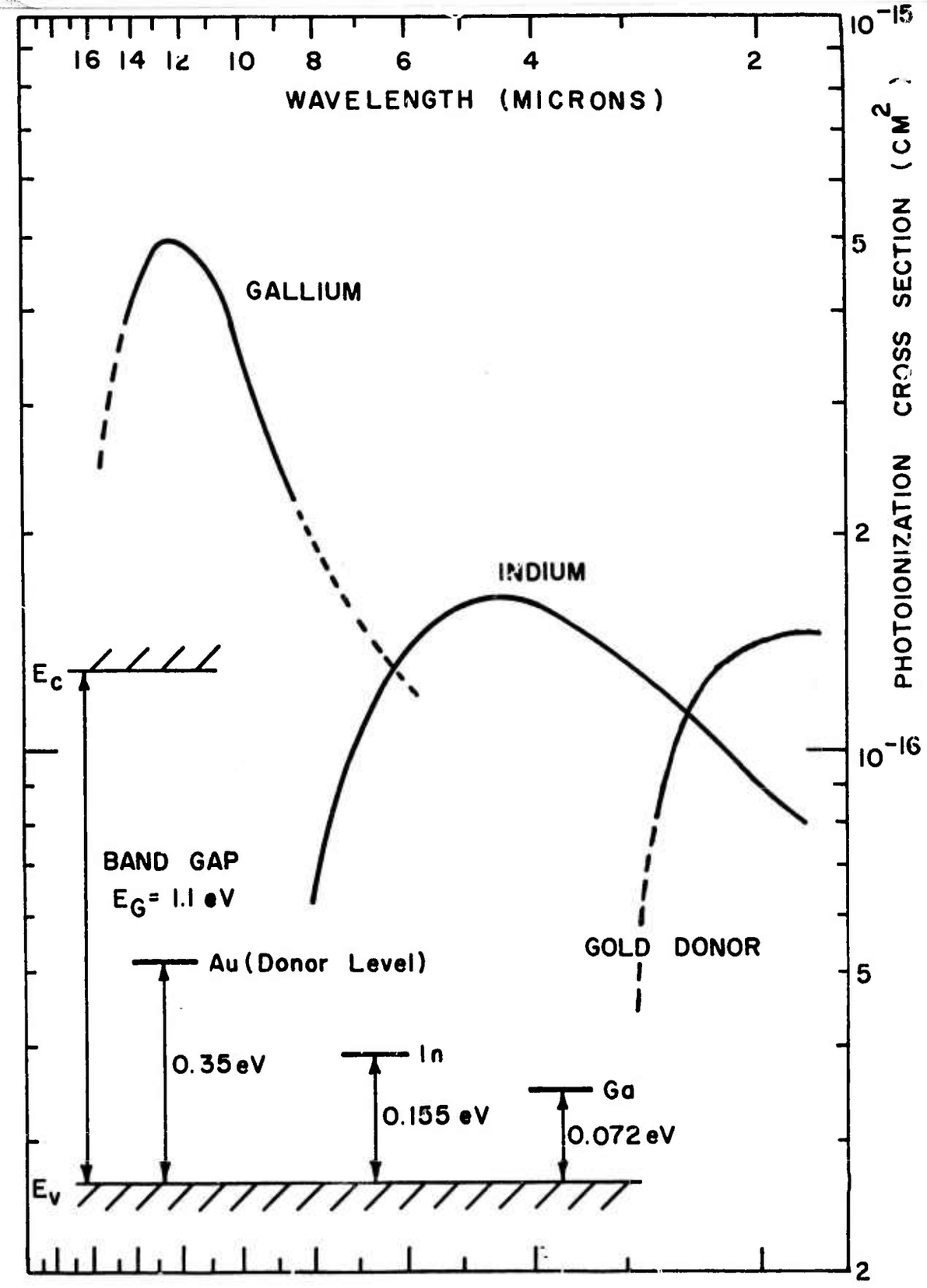

Fig. 16 Photoionization Cross Sections of Selected Impurities in Silicon

(iv) and the time constant of the decay depends only on the photoionization cross section and flux, there is good reason to believe the former is a constant dependent only on the type of impurity center.

Relatively high signal output powers for small total incident input energies are easily achieved. The devices are based upon silicon technology and it should be possible to construct large scale integrated arrays.

While at the current time, at least, we have investigated only the response of the gold-doped device in the near infrared, 1.0 to 3.0 microns, there would appear to be no reason why such response and this type of device might not be employed in the middle and for infrared wavelength ranges out to 14.0 microns by using indium and gallium doped devices.

Figure 16 shows the photoionization cross sections for indium, gallium and the gold donor level and their spectral dependencies. (1, 15). Current work is in progress to investigate indium doped devices and planned for gallium doped devices.

BIBLIOGRAPHY

(1) L. Forbes, and J. R. Yeargan, "Design for Silicon Infrared Sensing MOSFET," IEEE Trans. on Electron Devices, Vol. ED-21, No. 8, pp. 459-462, August, 1974.

(2) W. C. Parker, L.L. Wittmer, J. R. Yeargan, and L. Forbes, "Experimental Characterization of the Infrared Response of Gold-Doped Silicon MOSFET's (IRFET's)," Late News Paper 4.8, International Electron Device Meeting, Washington, D. C., December 9-11, 1974.

(3) C. T. Sah, The Equivalent Circuit Model in Solid-State Electronics-Part I: The Single Energy Level Defect Centers," Proceeding of the IEEE, Vol. 55 pp. 654-671, May 1967.

(4) C. T. Sah, L. Forbes, L.L. Rosier, and A. F. Tasch Jr., "Thermal and Optical Emission and Capture Rates and Cross Sections of Electrons and Holes from Photo and Dark Junction Current and Capacitance Experiments," Solid-State Electronics, Vol. 13, pp. 759-788, 1970.

(5) L. Forbes, "Thermal and Optical Emission and Thermal Capture of Electrons and Holes of Gold Centers in Silicon," Ph.D. Thesis, University of Illinois, 1970.

(6) C. T. Sah, L. Forbes, L.L. Rosier, A. F. Tasch, and A. B. Tole."Thermal Emission Rates of Carriers at Gold Centers in Silicon," Appl. Phys. Lett., Vol. 15, pp. 145-148, 1969.

(7) F. Hennig,"Emission and Capture of Electrons and Holes at Gold Centers in Silicon at Thermal Equilibrum," Ph.D. Thesis, University of Illinois, 1974.

(8) C. T. Sah, and H. S. Fu, "Current and Capacitance Transient Responses of MOS Capacitor, I. General Theory and Applications to Initially Depleted Surface without Surface States," Phys. Stat. Sol. (a), Vol. 11, pp. 297-310, 1972.

(9) C. T. Sah, and H. S. Fu, "Current and Capacitance Transient Responses of MOS Capacitor, Recombination Centers in Surface Space Charge Layer," Phys. Stat. Sol. (a), Vol. 14, pp. 59-70, 1972.

(10) R. H. Crawford, "MOSFET in Circuit Design," McGraw-Hill, New York, 1967.

(11) A. F. Tasch and C. T. Sah, "Recombination-Generation and Optical Properties of Gold Acceptor in Silicon," Physical Review B, Vol. 1, No. 2, pp. 800-809, 15 January 1970.

(12) S. Braun and H. G. Grimmeiss, "Thermal and Optical Generation Current in Reverse-Biased Gold-Doped Silicon P + N Junctions Without the Depletion Approximation," J. Appl. Phys., Vol. 44, No. 6, pp 2789-2794, June 1973.

(13) F. Grum, "Detector Intercomparison Results," Electro-Optical Systems Design, pp. 82-84, November, 1974.

(14) P. Richman, "The Effect of Gold Doping upon the Characteristics of MOS Field-Effect Transistors with Applied Substrate Voltage," Proc. of IEEE (Letters), Vol. 56, pp. 774-75, April 1968.

(15) H. B. Bebb, and R. A. Chapman, "Application of Quantum Defect Techniques to Photoionization of Impurities in Semiconductors," J. Phys. Chem. Solids, Vol. 28, pp. 2087-2097, 1967.